EUROPEAN COOPERATION
IN THE FIELD OF SCIENTIFIC
AND TECHNICAL RESEARCH

EURO-COST

SOURCE: UPC - Universitat Politècnica de Catalunya
UPV – Universidad Politécnica de Valencia

COST 2100 TD(10)11052
Aalborg, Denmark
2010/June/02-04

Link Abstraction Models Based on Mutual Information for LTE Downlink

Joan Olmos, Silvia Ruiz, Mario García-Lozano and David Martín-Sacristán*
Escola Politecnica Superior de Castelldefels (EPSC-UPC)
Esteve Terradas, 7. 08860 Castelldefels, SPAIN
*Universidad Politécnica de Valencia, iTEAM Research Institute
Camino de Vera, s/n. 46022 Valencia, SPAIN
Phone: +34 93 413 70 86
Fax: +34 93 413 70 07
Email: olmos@tsc.upc.edu

Link Abstraction Models Based on Mutual Information for LTE Downlink

Joan Olmos[1], Silvia Ruiz[1], Mario García-Lozano[1] and David Martín-Sacristán[2]

[1]Universitat Politècnica de Catalunya, WiComTec Group
{olmos,silvia,mariogarcia}@tsc.upc.edu
[2]Universidad Politécnica de Valencia, iTEAM Research Institute
damargan@iteam.upv.es

Abstract

In the context of LTE, link abstraction models are needed to condense the wideband channel quality measurements performed by the UE into a small set of Channel Quality Indicators (CQI). This paper studies two different link abstraction models focusing in the open-loop 2x2MIMO configuration specified for LTE downlink. The models, which are based on mutual information, are trained to obtain the relevant parameters and then tested on scenarios with different antenna correlation conditions. The results show that training a link abstraction model with a reduced bandwidth SISO system does not produce a set of parameters useful to predict the BLER of a 2x2 MIMO system of the same bandwidth under high antenna correlation. However, if link abstraction is trained with a 2x2 MIMO, zero forcing equalization, cyclic delay diversity and high antenna correlation, the obtained set of parameters are useful to estimate the BLER of a 2x2 MIMO with medium or low antenna correlation as well as the BLER of a SISO system.

Keywords

LTE, Link abstraction models, MIMO, Cyclic Delay Diversity

1. Introduction

3GPP Long Term Evolution (LTE) is the new standard that will make possible to deliver next generation mobile multimedia services with a quality similar to the obtained in current wired networks. To achieve this challenging goal, several important design decisions have been introduced. The radio access of LTE is called Evolved-UTRAN (E-UTRAN) and one of its main features is that all services, including real-time services, are supported over shared packet channels. This approach will achieve increased spectral efficiency, which will turn into higher system capacity with respect to current UMTS and HSPA. The use of packet access for all services also leads to better integration among all multimedia services and among wireless and fixed services. Low user-plane latency, defined as the Radio Access Network (RAN) round-trip delay, is important in order to achieve high bit-rate for data services. This low latency is partially achieved thanks to the specification of a Transmission Time Interval (TTI) of 1ms and because E-UTRAN is supported through a new packet core (Evolved Packet System, EPS) where all the user-plane radio related functionalities are placed at the Evolved-NodeB (eNB).

The radio interface of LTE uses Orthogonal Frequency Division Multiple Access (OFDMA) in the downlink (DL) and Single Carrier- Frequency Division Multiple Access (SC-FDMA) in the uplink (UL). Adaptive Modulation and Coding (AMC) is applied with three modulation schemes (QPSK, 16QAM and 64QAM) and variable coding rates. AMC allows delivering the desired throughput to the users at the cell border while achieving high spectral efficiency for users near the eNB. OFDM and SC-FDMA share some common features, like the easiness of modulation/demodulation by means of FFT, the use of a cyclic prefix (CP) to absorb the channel transient response between consecutive modulation symbols, the possibility of equalization in the frequency domain and easy integration with MIMO techniques. Frequency domain equalization is a key issue, since LTE radio-channels can use a bandwidth up to 20 MHz. OFDM shows inherent frequency diversity if a coded block is sent on a set of subcarriers spanning a bandwidth higher that the channel coherence bandwidth.

SC-FDMA, which has a lower Peak to Average Power Ratio (PAR) than OFDM, reduces the need for high linearity at the power amplifier of the User Equipment (UE).

Another key aspect of the LTE radio interface is the use of fast retransmission at the MAC level with incremental redundancy (H-ARQ). H-ARQ smoothes the AMC throughput curves, thus allowing less frequent switching between AMC formats.

MIMO techniques are well integrated into the LTE physical layer from the beginning. The MIMO schemes standardized for LTE include transmit diversity schemes as well as spatial multiplexing modes. Within the MIMO spatial multiplexing modes of LTE DL, a maximum of four spatial layers can be used but only two independent codewords can be transmitted. A codeword is a block of turbo encoded bits that is transmitted in one TTI. The eNB can use feedback from the UE in order to select a MIMO precoding matrix within a predefined set ("closed-loop" MIMO), or to rely on "open-loop" MIMO, where a fixed precoding matrix is applied. The precoding matrix can be seen as a set of adaptive complex weights applied at the eNB antenna ports aimed to improve the MIMO post-processing signal to noise ratio at the UE.

Even with open-loop MIMO, or with a transmission diversity scheme, feedback from the UE is always needed to perform Link Adaptation (LA). LA is the process by which the eNB, assisted by the UE, selects the Modulation and Coding Scheme (MCS) that will be used for DL transmission in the next TTI. LA aims to adapt the information data rate for each UE to its current channel capacity. In LTE the MCS is constant over all the allocated frequency resources of a particular user, but if two codewords are transmitted simultaneously using MIMO spatial multiplexing, then each codeword can use an independent MCS. The UE measures the DL received signal quality using the reference signals ("pilots") and reports to the eNB the preferred MCS for each codeword. This report is signaled using a Channel Quality Indicator (CQI) index, and summarizes the measured signal quality and also the UE capabilities since the UE is signaling a MCS such that, given current channel conditions, the next codeword can be received with a Block Error Rate (BLER) below 10%. Therefore, a suitable set of BLER vs. channel quality thresholds must be made available to the UE in order to produce meaningful CQI feedbacks. Here is where link abstraction models come into place, in order to obtain the set of valid Look up Tables (LUT) from which CQIs can be reported.

In LTE physical layer resources are structured in a time/frequency grid, where the minimum resources that can be allocated to a user are two Physical Resource Blocks (PRB) in two different slots of the same TTI. One PRB is equivalent to 12 subcarriers (180 kHz), during one slot (0.5ms). Taking into account that a single user transmission may use several PRBs and up to four spatial layers, to know the channel quality we need to measure the Signal to Interference plus Noise Ratio (SINR) in every subcarrier and every spatial layer. This is the situation in the so called "multi-state" channel. During transmission, the coded bits, which are spread over different subcarriers and spatial layers, experiment different fading conditions, and so we can not predict the BLER based on simple measurements.

A link abstraction model is a method to estimate the BLER experienced by a user under a multi-state channel in fast LA conditions, that is, when the TTI duration is less than the channel coherence time interval. In this situation, the traditional mean BLER vs. mean SINR curves are of little help to estimate the link performance. Notice that, in a SISO narrow-band channel, if the TTI is shorter than the channel coherence time the BLER could be estimated using the BLER curves for the involved MCS under AWGN assumption. A link abstraction model is also needed to perform fast resource scheduling at the eNB and, during system evaluations, to map from link level to system level simulations.

Link abstraction models for MIMO-OFDM systems have been studied recently by several authors, under general assumptions. One popular link abstraction model, recommended in [1] for system evaluation, is the Exponential Effective SINR Metric (EESM). In [2] several link abstraction models are compared in terms of the accuracy obtained in the BLER estimation. As a conclusion, the authors prove that the Mutual Information Effective SINR Metric (MIESM) outperforms EESM in terms of the BLER prediction accuracy. On the other hand, the MIESM method has the drawback that, since there is not a closed form expression for the Mutual Information (MI)

between transmitted and received modulation symbols, or between transmitted and received coded bits, it must be approximated or computed numerically. This paper focuses in the comparison of MIESM and EESM models for LTE DL in terms of complexity and BLER prediction accuracy. Emphasis is put on finding the model parameters that are suitable to predict the LTE DL BLER for a variety of physical layer configurations, ranging from SISO to MIMO in spatial multiplexing mode.

Link abstraction models usually must be trained, which means computing the set of model parameters that minimize the error between the real BLER and the estimated BLER. This task requires a Link Level simulator of LTE. To this purpose, an ad-hoc simulator written in C++, is also described and validated in this paper.

The rest of the paper is organized as follows. Section 2 describes the MIESM and EESM models. Section 3 describes the MI computation and gives the MI curves for QPSK, 16QAM and 64QAM. In Section 4 the LTE link level simulator is described and validated against results already available in the literature. Also in Section 4 the methodology used to train the link abstraction models is detailed. In Section 5 the simulation results are given and the different options for training MIESM and EESM are discussed, specifically for the LTE open-loop 2x2 MIMO spatial multiplexing mode under linear (Zero Forcing and MMSE) receivers.

2. Link Abstraction models: MIESM and EESM

As stated above, the new generation of cellular mobile communication systems and LTE also, work in packet mode using a wide-band radio channel. For pedestrian and low mobility scenarios, which is where MIMO spatial multiplexing techniques can be applied, the TTI of 1ms is shorter than the channel coherence time interval, and so the channel can be considered practically constant during the transmission of one Transport Block (TB) (the TB is the MAC layer PDU in LTE and, except for large TB sizes, it is mapped to a single codeword). Under this assumption, the BLER can be estimated using the AWGN hypothesis, but an additional many-to-one mapping function is needed to map form the multiple SINR measurements available in the multi-state channel to one or two scalars that can finally be used to estimate the BLER. As proposed in [3], we will use a single scalar to summarize the whole set of multi-state channel quality measurements. This leads to the concept of Effective SNR (ESNR).

Given an experimental BLER measured in a multistate channel with a specific MCS, the ESNR of that channel is defined as the SNR that would produce the same BLER, with the same MCS, in AWGN conditions. As explained in [2], for a given multistate channel with N different SINR measurements $\{\gamma_1, \gamma_2 ... \gamma_N\}$, the ESNR can be estimated as the value γ_{eff} that accomplishes the equation:

$$I\left(\frac{\gamma_{eff}}{\alpha_1}\right) = \frac{1}{N}\sum_{k=1}^{N} I\left(\frac{\gamma_k}{\alpha_2}\right) \quad (1)$$

Where the function $I(\cdot)$ can take several forms, and the constants α_1 and α_2 are model parameters that can be adjusted to minimize the error between the BLER predicted by the model and the experimental BLER. As can be seen in exp. (1), the function $I(\cdot)$ is used to calculate a weighted average of the individual SINR measurements after being previously scaled by α_2. The objective of the $I(\cdot)$ function is to estimate the amount of information that can be delivered by a modulation symbol at a given SNR. For an M-QAM modulation at high SNR this is bounded by $log_2 M$ bits.

In the MIESM model the function $I(\cdot)$ is the MI between the transmitted and received modulation symbols vs. SNR in AWGN, [4]. This function is modulation specific, although the main difference from QPSK to 16QAM and from 16 to 64QAM is a SNR shift of about 5dB. Fig. 1 shows the MI, normalized by the number of bits per modulation symbol (average MI at bit level, MIB), for the three modulation schemes used in LTE. Fig. 1 shows also the function *1-exp(-SNR)*, which is very similar to the MIB for QPSK with a SNR shift of 1.8dB.

The EESM model uses the function $I(\gamma)=1-exp(-\gamma)$ for all the modulation schemes, and in many cases the constants α_1 and α_2 are taken to be equal, i.e. $\alpha_1 = \alpha_2 = \beta$. Refs. [5] and [3] provide a derivation of the EESM model. The parameter β can be interpreted as a shift in the $I(\cdot)$ function to adapt the model to the different MCS.

If a MIMO multiplexing scheme is applied, assuming that linear processing (Zero Forcing or MMSE) is in use at the receiver, we still can use the ESNR concept by taking the MIMO post-processing SINR as the set of measurements $\{\gamma_1, \gamma_2 ... \gamma_N\}$ of the multi-state channel. Assuming that the receiver has a good estimation of the MIMO matrix channel, it can compute the post-processing SINR based on well known expressions.

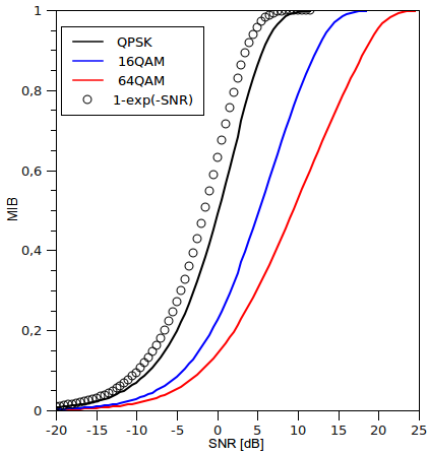

Fig. 1 MIB for the LTE modulation schemes

In MIMO spatial multiplexing the antenna correlation is translated into degradation of the post-processing SINR, so assuming again that the channel is known, the ESNR model may also capture the effect of antenna correlation. The parameters α_1 and α_2 depend on the modulation scheme, the code block size and the code rate but should be valid for SISO and MIMO with linear equalization regardless of the MIMO antenna correlation level.

It is known that in line of sight (LoS) propagation scenarios, which can be favorable for MIMO spatial multiplexing, the channel exhibits high SNR values but also high antenna correlation. In order to fight the antenna correlation, in the case of 2x2 open-loop MIMO in spatial multiplexing mode, the LTE specifications dictate the use of a fixed precoding matrix and a Cyclic Delay Diversity (CDD) scheme in the eNB, [6]. Since all this processing can be included inside a modified matrix channel, the receiver can equalize the eNB processing and the channel as a whole, and again all the effects, including precoding and CDD at the eNB, are properly captured by the post-processing SINR and by the ESNR model.

3. *Computation of the Mutual Information*

The MI for two random variables x, y is defined as:

$$MI(x,y) = E_{x,y}\left[log_2\left(\frac{f_{y|x}(y|x)}{f_y(y)}\right)\right] \quad (2)$$

Where $E_{x,y}(\cdot)$ means expectation over $\{x,y\}$, $f_{y|x}(y|x)$ is the conditional probability density function (p.d.f.) of $y|x$, and $f_y(y)$ is the p.d.f. of y. If we take x to be the transmitted M-QAM modulation symbol and y the received decision variable, the $MI(x,y)$ can be written as:

$$MI(x,y) = \frac{1}{M}\sum_{i=1}^{M} E_{y|x_i}\left[log_2\left(\frac{f_{y|x_i}(y|x_i)}{f_y(y)}\right)\right] \quad (3)$$

The Log-Likelihood Ratio (LLR) at modulation symbol level for a modulation with M states is defined as:

$$LLR_{x_i}(y) = log_e\left(\frac{P(x_i|y)}{\sum_{k=1;k\neq i}^{M} P(x_k|y)}\right) \quad (4)$$

Where $P(x_i|y)$ means the probability that state x_i has been transmitted given that the received decision variable is y. Assuming equal transmission probabilities for all modulation symbols, it's easy to prove that:

$$\frac{f_{y|x_i}(y|x_i)}{f_y(y)} = \frac{M}{1+e^{-LLR_{x_i}(y)}} \quad (5)$$

And so, exp. (3) can be written as:

$$MI(x,y) = \frac{1}{M}\sum_{i=1}^{M} E_{y|x_i}\left[log_2\left(\frac{M}{1+e^{-LLR_{x_i}(y)}}\right)\right] \quad (6)$$

Notice that, for high SNR the LLRs are much larger than 1 and so exp. (6) tends to $log_2 M$. Again, assuming equal transmission probabilities for all modulation symbols and AWGN channel, exp. (4) becomes:

$$LLR_{x_i}(y) = log_e\left(\frac{e^{-d_i/\sigma^2}}{\sum_{k=1;k\neq i}^{M} e^{-d_k/\sigma^2}}\right) \quad (7)$$

Where d_i is the distance from decision variable y to symbol x_i and σ is the noise variance. Using expressions (6) and (7) the MI can be computed numerically by means of a simulator. The computation involves creating high resolution histograms of the symbol level LLRs, then normalize the histograms to get the p.d.f. of the LLRs and finally perform the averaging operation in exp. (6) by numerical integration. In general, and depending on the modulation scheme, the different symbols have different LLR statistics. In Fig. 2 the p.d.f. of the LLRs for the symbol in the bottom left corner of the constellation is shown for the LTE modulation schemes. In [3] an approximated closed form expression for the MI in BPSK is given. The curves of MI for the LTE DL modulation schemes are given in Fig. 1.

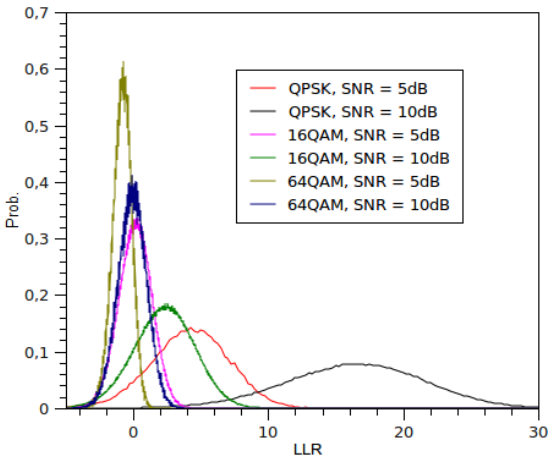

Fig. 2 p.d.f. of the LLRs for the LTE modulation schemes

4. E-UTRA DL simulator

4.1. Simulator description

In order to train and test the different link abstraction models for LTE, an ad-hoc E-UTRA link level simulator has been programmed in C++ language. The E-UTRA link level simulator features an OFDM physical layer in accordance with [7] and [8]. In Fig. 3 a block diagram of the DL simulator MIMO 2x2 configuration is depicted.

The rate 1/3 turbo encoder with variable code block size creates three independent streams with systematic and redundant bits. These streams are interleaved and fed to the circular buffer rate matching and H-ARQ procedure. Variable coding rate is achieved by applying different puncturing patterns depending on the current H-ARQ redundancy version (RV). Up to four incremental redundancy (IR) transmissions per code block are allowed. The turbo decoder uses a MAP algorithm and a maximum of 8 decoding iterations. ACK/NACK error free transmission is considered.

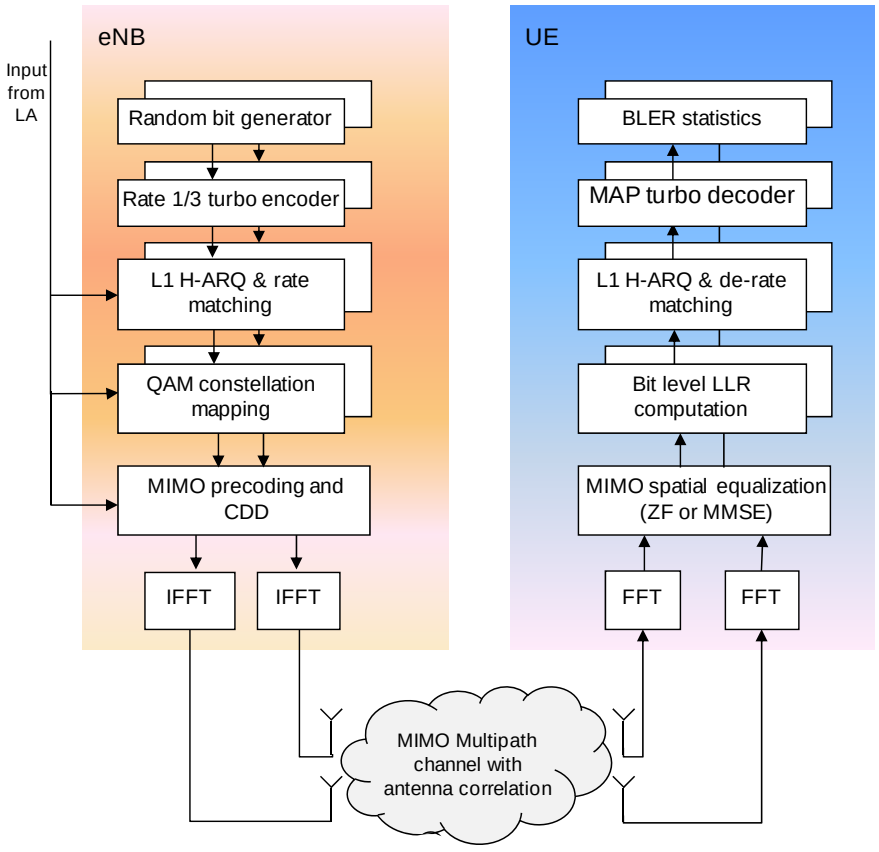

Fig. 3 Block diagram of the E-UTRA DL simulator

The QAM modulator generates the complex modulated symbols, belonging to either a QPSK, 16QAM or 64QAM constellation. Signaling and pilot symbols overhead is not considered. If the MIMO 2x2 configuration is simulated, then the turbo encoding, rate matching and modulation procedures are repeated for the second spatial layer with an independent input bit stream.

The LTE specifications include a fixed precoding matrix and CDD at the eNB in the open-loop 2x2 MIMO transmission mode. CDD consists in transmitting the same OFDM symbols on the same set of subcarriers from multiple antennas with a different delay on each antenna. This creates an artificial multipath that translates into

additional frequency diversity, which is then exploited by the turbo code. Since the delay is introduced before adding the CP it can be higher than the CP duration. The delay can be implemented as a cyclic shift of the time domain samples after the IFFT or as a subcarrier dependent phase rotation. From this point of view, CDD can be seen as an additional subcarrier dependent precoding matrix, and so it forms part of the global matrix channel to be equalized at the UE. The vector to transmit on subcarrier *k* from the two antenna ports, $\vec{\boldsymbol{v}}(\boldsymbol{k})$, given two modulated symbols $x_0(i)$ and $x_1(i)$ is obtained as:

$$\vec{v}(k) = \begin{bmatrix} v_0(k) \\ v_1(k) \end{bmatrix} = \frac{1}{\sqrt{2}} \begin{bmatrix} 1 & 0 \\ 0 & e^{j\pi k} \end{bmatrix} \begin{bmatrix} 1 & 1 \\ 1 & -1 \end{bmatrix} \begin{bmatrix} x_0(i) \\ x_1(i) \end{bmatrix} \tag{8}$$

It can be observed in (8) that the cyclic delay is equivalent to half the OFDM symbol period, and that antenna port *0* is fed with $x_0(i)+x_1(i)$ and port *1* with $x_0(i)-x_1(i)$ for even subcarriers or $x_1(i)-x_0(i)$ for odd subcarriers. The received vector $\vec{y}(k)$ on subcarrier *k* is:

$$\vec{y}(k) = \begin{bmatrix} h_{11} & h_{12} \\ h_{21} & h_{22} \end{bmatrix} \vec{v}(k) + \vec{n} = \frac{1}{\sqrt{2}} \begin{bmatrix} h_{11} + h_{12}e^{j\pi k} & h_{11} - h_{12}e^{j\pi k} \\ h_{21} + h_{22}e^{j\pi k} & h_{21} - h_{22}e^{j\pi k} \end{bmatrix} \begin{bmatrix} x_0(i) \\ x_1(i) \end{bmatrix} + \vec{n} \tag{9}$$

and even if $h_{11} \cong h_{12}$ and $h_{21} \cong h_{22}$ (high correlation on the UE side) only the symbol $x_1(i)$ is highly degraded for even subcarriers, but not for odd subcarriers where the roles of $x_0(i)$ and $x_1(i)$ are interchanged.

The MIMO matrix channel is generated in time domain with the desired correlation properties. We generate each matrix element impulse response using a classical stochastic tapped delay line model and all matrix elements share the same power delay profile (PDP), [11]. In the frequency domain the received vector on subcarrier *k* is:

$$\vec{y}(k) = \left(\sum_{i=1}^{n} [H]_{\mathrm{i}} \, e^{-j2\pi k \Delta f \tau_i} \right) \vec{v}(k) + \vec{n} \tag{10}$$

where *n* is the number of taps and $\boldsymbol{\Delta f}$ is the carrier spacing (15kHz). Matrixes $[\boldsymbol{H}]_{\mathbf{i}}$, which model the multipath, are 2x2 complex time variant matrixes and delays $\boldsymbol{\tau_i}$ are constant. The number of taps, the delays $\boldsymbol{\tau_i}$ and the power of matrixes $[\boldsymbol{H}]_{\mathbf{i}}$ depend on the simulated PDP. The Doppler spectrum of the different taps is shaped by a classical Jakes low-pass filter.

Correlation among antennas is introduced using the procedures recommended in [11]. Based on this assumption, the spatial correlation matrix of the MIMO matrix channel is the Kronecker product of the spatial correlation matrixes at the eNB and UE:

$$R_{spat} = R_{eNB} \otimes R_{UE} = \begin{bmatrix} 1 & \alpha \\ \alpha^* & 1 \end{bmatrix} \otimes \begin{bmatrix} 1 & \beta \\ \beta^* & 1 \end{bmatrix} = \begin{bmatrix} 1 & \beta & \alpha & \alpha\beta \\ \beta^* & 1 & \alpha\beta^* & \alpha \\ \alpha^* & \alpha^*\beta & 1 & \beta \\ \alpha^*\beta^* & \alpha^* & \beta^* & 1 \end{bmatrix} \tag{11}$$

Ref. [11] also specifies three different levels of antenna correlation, termed low, medium and high correlation level. For low correlation $\alpha = \beta = 0$, for medium correlation $\alpha = 0.3$; $\beta = 0.9$, and for high correlation $\alpha = \beta = 0.9$. Matrixes $[H]_{\mathrm{i}}$ are initially generated with i.i.d. elements and then those elements are correlated using Cholesky factorization.

Ideal channel estimation is assumed for MIMO equalization, which is based on ZF or MMSE. Although H-ARQ can also be simulated, it is not relevant in this study since the CQI is selected based on the BLER for the first RV.

4.2. Validation of AWGN Reference BLER curves for the LTE CQIs

In order to train the link abstraction models the reference BLER curves in AWGN must be obtained. This curves are obtained in SISO mode and using the table from [10] which specifies the MCS for each CQI. This result can also be used to validate the simulator, at least in SISO mode, against previously published results in the literature. The set of reference BLER curves is dependent on the bandwidth allocated to the user, since the more PRBs are available the higher is the turbo code block size that can be applied. There is a finite set of valid turbo code block sizes, as specified in [8], which range from 40 bits to 6144 bits. In LTE the PRBs are allocated in groups called a Resource Block Grup (RBG), where the number of PRBs in a RBG depends on the system bandwidth. For a system bandwidth lower that 11 PRBs the size of a RBG is 1 PRB, while for a system bandwidth higher than 63 PRBs the size of a RBG is 4 PRBs.

Fig. 4 shows the obtained reference BLER curves in AWGN for RBG=1 and RBG=4. The curves are spaced by 2 dB approximately.

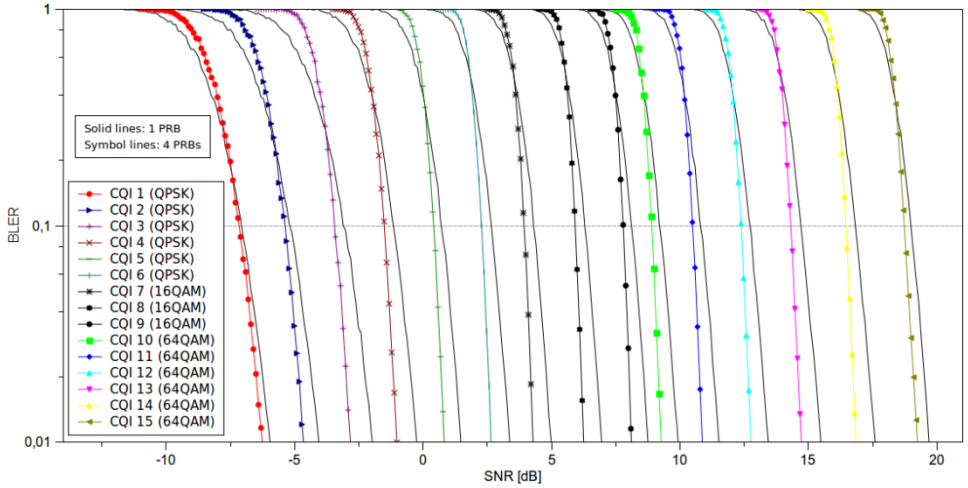

Fig. 4 LTE DL AWGN Reference BLER (RV=0) vs. SNR for SISO configuration and RBG sizes=1 and 4

It can be verified that these curves show good agreement with previously published results in [1] and [6]. The BLER curves for RBG=4 show a steeper slope due to the larger code block sizes. The horizontal line at BLER=10% defines the set of SNR thresholds to compare with the current channel ESNR and select the highest CQI compatible with a BLER<10%.

4.3. Validation of LTE open loop MIMO 2x2 with CDD

Assuming a MIMO system with *N* Tx antennas and *M* Rx antennas, for ZF the post-processing SINR of spatial layer *i* at subcarrier *k* is:

$$SINR_{i,k}^{ZF} = \frac{\overline{|C_k|^2}}{\sigma^2 \left[[H]^H [H] \right]_{i,i}^{-1}} \tag{12}$$

where $\overline{|C_k|^2}$ is the transmitted signal power on port *i* and subcarrier *k*, σ^2 is the receiver complex noise power in a subcarrier bandwidth, $[H]$ is the *MxN* channel matrix, $[\cdot]^H$ means conjugate transpose matrix and $[\cdot]_{i,i}^{-1}$ means the *i* diagonal element of the inverse matrix. With the same notation, the post-processing SINR for MMSE is, [14]:

$$SINR_{i,k}^{MMSE} = \frac{\frac{\overline{|C_k|^2}}{\sigma^2}}{\left[\frac{\sigma^2}{|C_k|^2}[I_N] + [H]^H[H]\right]_{i,i}^{-1}} - 1 \tag{13}$$

The effects of CDD can be observed by plotting the ZF post-processing SINR for the whole set of subcarriers. Fig. 5 is such a plot for 2x2 MIMO (64QAM) with bandwidth = 4 PRBs in EPA channel. Without antenna correlation there is little difference in the codeword SINR with or without CDD. With high antenna correlation and no CDD both codewords show very low SINR, but with CDD the SINR alternates between good and bad every two subcarriers. This is exploited by the turbo code, which is able to average between good and bad subcarriers and obtain a better performance than without CDD. CDD is especially important in pedestrian environment, since the channel shows poor frequency selectivity as shown in Fig. 5. In the same figure it can be verified that CDD introduces high dynamics in the post-processing SINR vs. frequency (more that 10dB in this example).

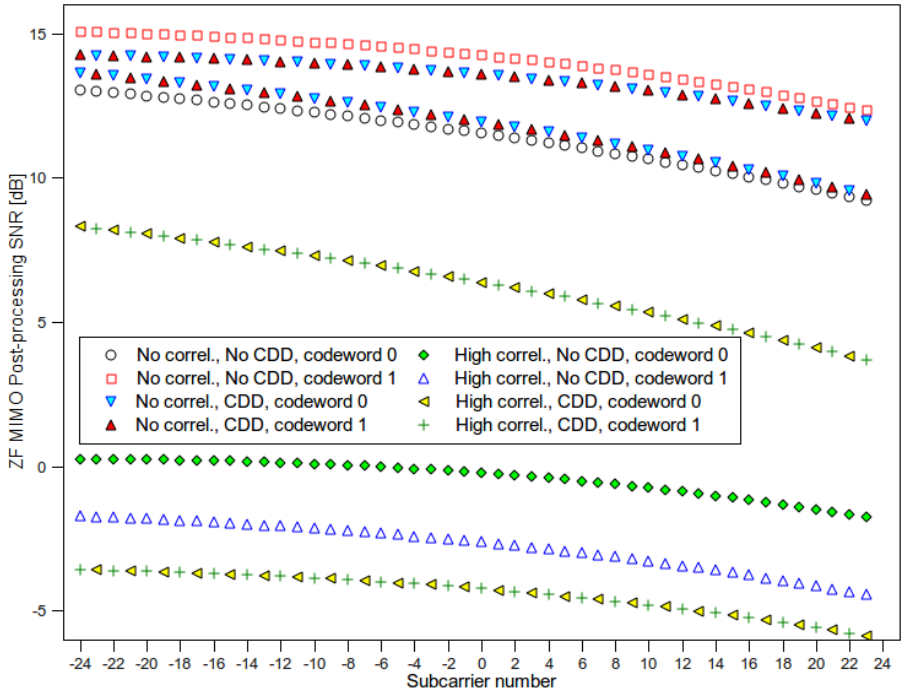

Fig. 5 Post-processing SINR for ZF open-loop 2x2 MIMO (64QAM) with bandwidth = 4 PRBs and EPA channel

To validate the MIMO implementation of the simulator Fig. 6 shows the uncoded BER for a 2x2 MIMO with ZF equalization. Since the BER is the same for the two spatial layers, only one layer is shown. The modulation is 16QAM and the allocated bandwidth is 4 PRBs. The PDP corresponds to the EPA channel, [11], and the mobile speed is 3km/h.

Assuming uncorrelated antennas, it is known that the performance of a *NxM* MIMO system in spatial multiplexing mode with ZF processing equals that of a system with Maximal Ratio Combining (MRC) with one Tx antenna (sending with the same power as a Tx antenna of the ZF MIMO system) and *M–N+1* Rx antennas, [12]. For a 2x2 situation this means diversity order=1; so the expected performance, in terms of the uncoded BER, is the same as that of a SISO 16QAM system in Rayleigh fading.

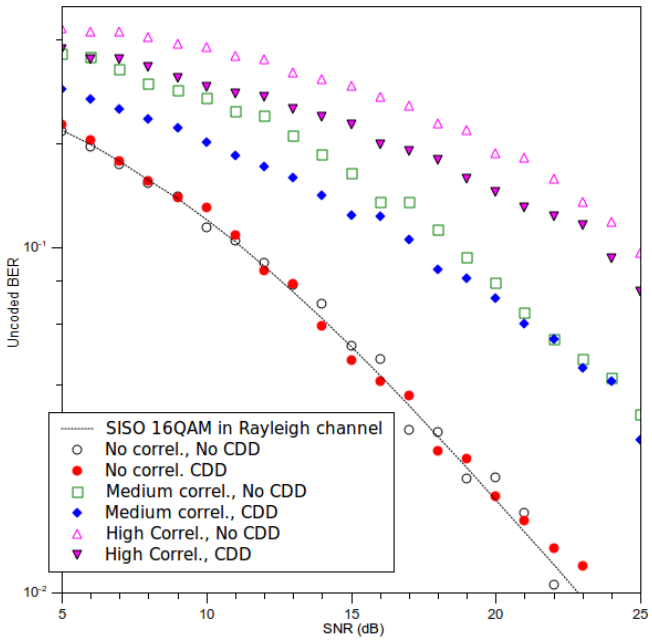

Fig. 6 Uncoded BER for ZF open-loop MIMO 2x2 (16QAM) with bandwidth = 4 PRBs and EPA channel @ 3km/h

In Fig. 6 we can verify that there is a very good agreement between the simulated uncoded BER and the theoretical BER curve for SISO 16QAM in Rayleigh fading. The theoretical BER of 16QAM in Rayleigh fading has been obtained from [13].

Fig. 6 also shows the uncoded BER, with and without CDD, for the different antenna correlation levels. It can be noticed that CDD does not degrade the performance in the absence of antenna correlation, but it can introduce a gain of up to 4 dB in the uncoded BER with high antenna correlation.

4.4. Training methodology of link abstraction models

Once we have calculated the reference BLER curves in AWGN, the next step is to train the link abstraction models, that is, to find the most adequate parameters in exp. (1). In general, a different set of parameters is needed for every MCS and code block size. To estimate the link abstraction model parameters the simulator is used to generate a large number of snapshots of the MIMO multipath channel. Every channel snapshot is characterized by a set of SINR measurements $\{\gamma_1^i, \gamma_2^i \dots \gamma_N^i\}$ where γ_k^i $(k = 1,2..N)$ denotes the post-processing MIMO SINR for spatial layer *0*, subcarrier *k* and snapshot *i*. Since in open-loop both spatial layers show the same performance, and in 2x2 MIMO each codeword uses a different layer, the SINR measurements can be taken only from layer *0*, for example. For each instance of the MIMO channel a large number (10000) of code blocks are simulated and a BLER measurement for the snapshot *i* ($BLER_i$) is obtained. The MIMO matrix channel remains constant during the simulation of a given channel snapshot. Depending on the MCS, a careful adjustment of the simulated mean SNR is needed to obtain values of $BLER_i$ that are in a range from 0.01 to aprox. 0.9, since a BLER outside this range is of no interest for the purposes of training the model. The number of simulated snapshots must be as high as possible, but in order to limit the simulation time we have used a number of snapshots between 100 and 200.

For EESM in the one dimension case, that is when $\alpha_1 = \alpha_2 = \beta$, the ESNR of the snapshot *i* is expressed as a function of the unknown β, i.e.:

$$\gamma_{eff}^{i}(\beta) = -\beta \, log_e\left(\frac{1}{N}\sum_{k=1}^{N} e^{-\frac{\gamma_k^i}{\beta}}\right) \tag{14}$$

then, if we call M to the number of simulated snapshots, the value of β is obtained as:

$$\beta = \arg_{\min}\left\{\sum_{i=1}^{M}\left[log_{10}(BLER_i) - \, log_{10}\left(BLER_R(\gamma_{eff}^{i}(\beta))\right)\right]^2\right\} \tag{15}$$

where $BLER_R(\cdot)$ is the reference BLER curve in AWGN channel for the current MCS and code block size. That is, to obtain β we minimize the mean squared error between the estimated BLER and the simulated BLER for the set of simulated snapshots using numerical methods. By using the logarithmic BLER error in (15) the minimization algorithm tries to obtain low error at low BLER, which is the region of interest.

For MIESM exp. (14) must be substituted by:

$$\gamma_{eff}^{i}(\alpha_1;\alpha_2) = \alpha_1 \, I^{-1}\left(\frac{1}{N}\sum_{k=1}^{N} I\left(\frac{\gamma_k^i}{\alpha_2}\right)\right) \tag{16}$$

and the calculation of α_1 and α_2 involves a bi-dimensional minimization of the mean square error (MSE):

$$MSE(\alpha_1;\alpha_2) = \sum_{i=1}^{M}\left[log_{10}(BLER_i) - \, log_{10}\left(BLER_R(\gamma_{eff}^{i}(\alpha_1;\alpha_2))\right)\right]^2 \tag{17}$$

With the additional difficulty that the MI function, $I(\cdot)$, must be inverted numerically.

5. Results

Next sections present the results concerning the training of MIESM and EESM models with the simulator described in section 4. Table 1 is a summary of the most relevant parameters considered in the simulations.

Table 1. Summary of simulation parameters

Parameter	Value
Carrier frequency	2.14 GHz
Simulated Bandwidth	720 kHz
Subcarrier spacing	15 kHz
FFT size	64
Number of useful subcarriers	48
Number of subcarriers per PRB	12
Number of allocated PRBs	4
TTI interval	1 ms
Number of useful OFDM symbols per TTI	11
Power Delay Profile	EPA channel model at pedestrian speed (3 km/h) for MIMO and ETU for SISO [9]
Channel Coding	Turbo code basic rate 1/3
Rate Matching	According to [8]
MCS formats	As specified in [10] for each of the 15 possible CQI indexes
Channel estimation	Ideal
Antenna scheme	SISO and 2x2 MIMO

5.1. Finding optimum parameters for MIESM in 2x2 MIMO configuration

In this section, the optimum parameters, α_1 , α_2 are found for the MIESM models in a 2x2 open-loop MIMO configuration. In order to get parameters valid for any degree of antenna correlation, it seems adequate to start by training the models with BLER results in EPA channel, CDD and high antenna correlation (HC). The reason is that, as shown in previous section, CDD and ZF create high dynamics in the post-processing SINR and so the model is trained with a big variety of SINR measurements. Deep frequency selective fading could also be obtained by training the model with a channel with higher delay spread, like ETU [11] for example, but CDD is even better to this purpose because half of the subcarriers are in fading with respect to the other half. Before starting the numerical bi-dimensional minimization algorithm, an exhaustive search has been performed in a wide range of the α_1 , α_2 parameters. The MIESM MSE vs. α_1 , α_2 (in dB) is shown in Fig. 7 for CQI 1 and CQI 11 for MIMO HC situation. This procedure allows feeding the minimization algorithm with a good initial guess.

The dots in Fig. 8 show the BLER for the simulated channel snapshots vs. the ESNR of the snapshot for the different CQIs. The solid lines are the reference BLER curves in AWGN. The simulation conditions for Fig. 8 are: HC MIMO (ZF) with CDD in a bandwidth of 4 PRBs and EPA channel. A good agreement is found between the MIESM estimated BLER and the reference curves. Table 2 lists the obtained MIESM parameters as well as the MSE for each CQI. The size of the code block and the approximated code rate for each CQI are also included as a reference. The code block size is the largest size that produces a codeword that fits in the available bandwidth of 4 PRBs taking into account that there are 11OFDM useful blocks per TTI (3 OFDM blocks per TTI are used for control channels).

Table 2. MIESM parameters and MSE for all the CQIs in a bandwidth of 4 PRBs

CQI	Code block size	Approx. code rate	α_1	α_2	MSE
1	72	0,072	0,278	0,276	0,002
2	112	0,113	0,389	0,385	0,003
3	192	0,185	0,633	0,629	0,002
4	312	0,297	1,056	1,067	0,008
5	456	0,435	1,111	1,112	0,045
6	608	0,585	1,035	1,019	0,013
7	768	0,368	1,065	1,121	0,002
8	1008	0,477	1,034	1,065	0,008
9	1248	0,600	0,937	0,980	0,013
10	1440	0,455	0,942	1,150	0,008
11	1728	0,553	0,556	0,727	0,010
12	2048	0,650	0,700	0,935	0,017
13	2368	0,753	0,760	1,017	0,038
14	2688	0,852	0,657	0,821	0,006
15	2880	0,925	0,840	0,985	0,024

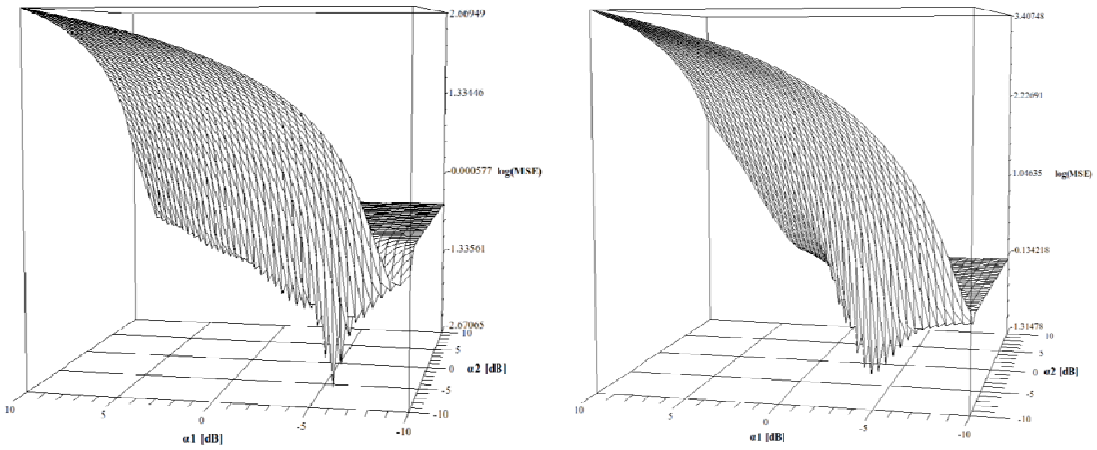

Fig. 7 HC MIMO MIESM MSE vs α_1, α_2 for CQI 1 (left) and CQI 11(right)

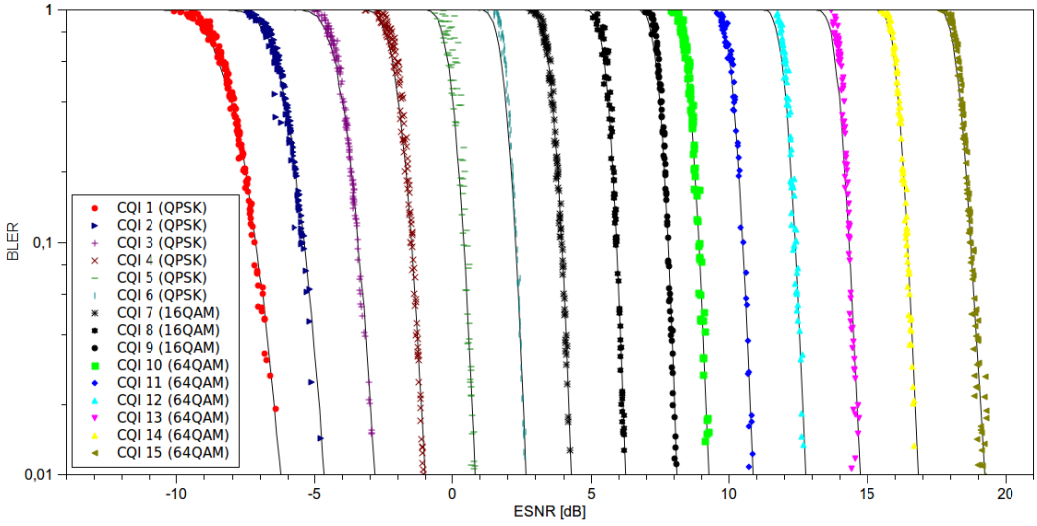

Fig. 8 MIESM estimated BLER vs ESNR for HC MIMO (ZF) with CDD in a bandwidth of 4 PRBs and EPA channel

Fig. 9 compares the obtained MIESM MSE with the MSE obtained by simplifying the problem to a one-dimension minimization. This can be done by setting $\alpha_1 = \alpha_2$, $\alpha_2=1$, or simply taking $\alpha_1 = \alpha_2=1$ for no minimization at all. It can be seen that the best results are obtained always with bi-dimensional minimization, and that taking $\alpha_1 = \alpha_2$ is not a bad approach for QPSK and 16QAM but it produces high error with 64QAM.

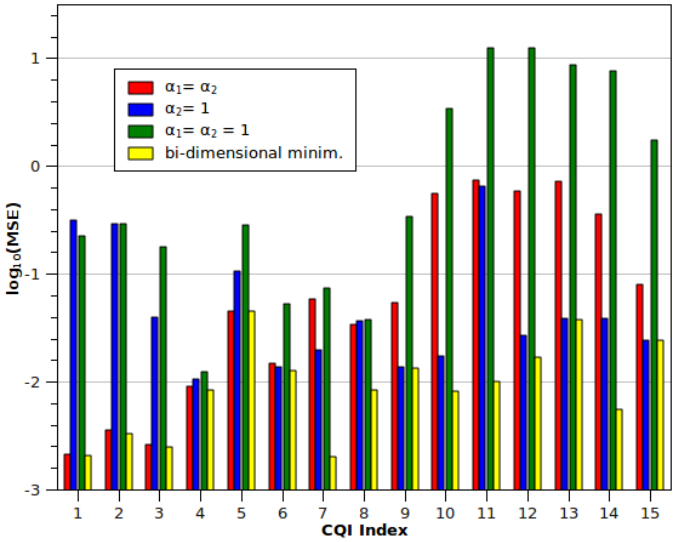

Fig. 9 Comparison of MIESM MSE with bi-dimensional vs. one-dimension minimization

Now, the MIESM parameters obtained under MIMO in HC conditions can be applied to predict the BLER in situations with no antenna correlation (NC) or medium antenna correlation (MC). Assuming the system configuration of 2x2 ZF MIMO, the obtained MSE is compared in Fig. 10 with the minimum MSE (obtained by training the model with the NC or MC scenario respectively). The MSE is low and close to the minimum that can be obtained.

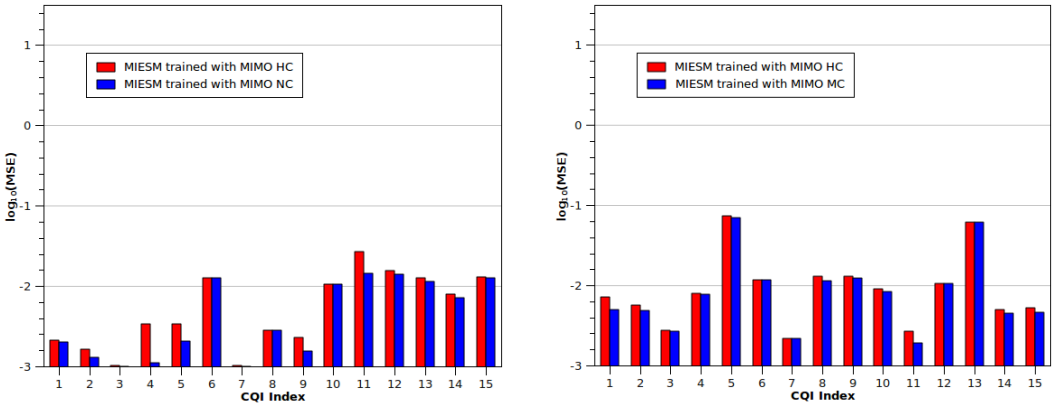

Fig. 10 Comparison of MIESM MSE in MIMO with medium(right) or no antenna correlation(left) when training the model in MIMO HC

It has been also verified that MIESM parameters obtained under MIMO ZF in HC conditions can be used to predict the BLER in a MMSE equalized MIMO and in a SISO system (see Fig. 11) . However, the reverse situation does not hold. Fig. 12 compares the MIESM MSE when trying to predict the BLER in a MIMO HC scenario using MIESM parameters trained with a SISO system, with the same bandwidth, under ETU channel (ETU was used with SISO to increase the frequency selectivity of the fading). The MSE error of the SISO trained model is much higher than that of the model trained in MIMO HC. This does not mean that MIESM can not be trained using a SISO simulator, but rather than in order to obtain valid MIESM parameters with SISO the simulator must use a bandwidth wider than 4 PRBs, so that channel snapshots contain a larger set of different SINR values.

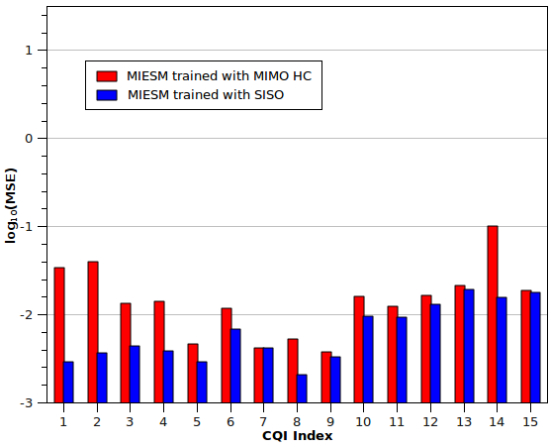

Fig. 11 Comparison of MIESM MSE in a SISO system when training the model in MIMO HC

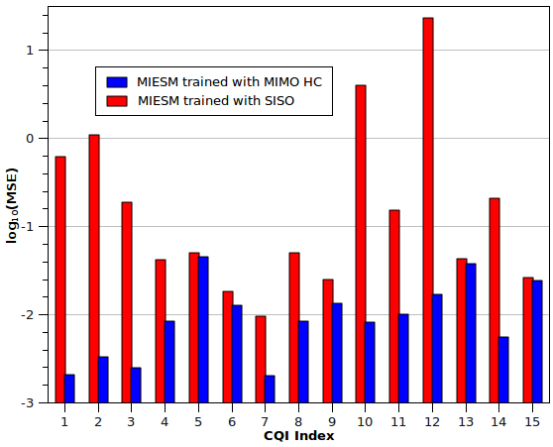

Fig. 12 Comparison of MIESM minimum MSE in MIMO HC when training the model with a SISO system in ETU channel

5.2. Finding optimum parameters for EESM in 2x2 MIMO configuration

The main advantage of EESM over MIESM is that the non-linear weighting function, $I(\cdot)$, used to calculate the ESNR is very easy to compute in forward and inverse directions. The performance of EESM to predict the BLER in the MIMO HC scenario has been tested in two ways: using a single parameter (one-dimension minimization) or using two different parameters. The advantage of using a single parameter is that minimization is simple and there is a single minimum, as shown in Fig. 13 for CQI 14, although the MSE can be quite flat in some regions of β. The minimum MSE with single parameter EESM is high for 64QAM, as shown in Fig. 14, and so using a single parameter for EESM is not a general solution. This is in agreement with previously published results for a SISO system in [15]. Fig. 14 shows also that using two parameters for EESM gives much lower MSE for 64QAM than using a single parameter, although by comparing the blue bars in Fig. 14 with those in Fig. 12 it's clear that MIESM still outperforms EESM. Table 3 lists the obtained EESM parameters as well as the MSE for each CQI. The values of β are in good agreement with those previously published in [5] for QPSK and 16QAM. Fig. 15 plots the EESM (with dual parameter) estimated BLER for the simulated channel snapshots on top of the reference BLER curves.

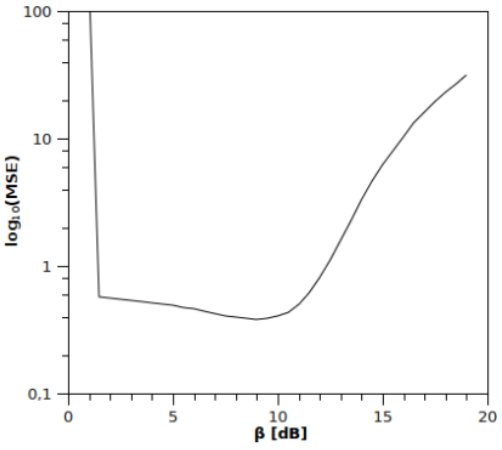

Fig. 13 EESM MSE vs. β in MIMO HC for CQI 14

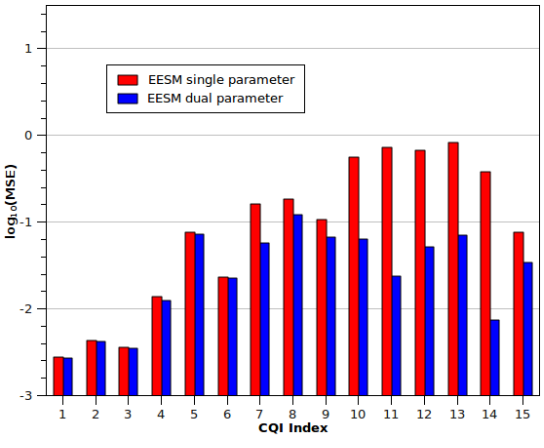

Fig. 14 EESM minimum MSE in MIMO HC for all CQIs

Table 3. EESM parameters and MSE for all the CQIs in a bandwidth of 4 PRBs

CQI	Code block size	Approx. code rate	β	MSE	α_1	α_2	MSE
1	72	0,072	0,372	0,003	0,363	0,360	0,003
2	112	0,113	0,531	0,004	0,519	0,515	0,004
3	192	0,185	0,865	0,004	0,858	0,855	0,003
4	312	0,297	1,403	0,014	1,439	1,460	0,012
5	456	0,435	1,636	0,076	1,647	1,675	0,073
6	608	0,585	1,646	0,023	1,636	1,621	0,022
7	768	0,368	3,418	0,159	3,748	4,123	0,057
8	1008	0,477	5,042	0,182	5,160	5,491	0,121
9	1248	0,600	6,122	0,106	6,307	6,649	0,066
10	1440	0,455	1,010	0,553	9,790	12,262	0,064
11	1728	0,553	0,399	0,713	11,489	14,827	0,024
12	2048	0,650	0,621	0,658	17,669	23,625	0,051
13	2368	0,753	0,962	0,825	24,081	32,971	0,069
14	2688	0,852	7,933	0,382	22,622	28,049	0,007
15	2880	0,925	15,859	0,077	25,245	28,103	0,034

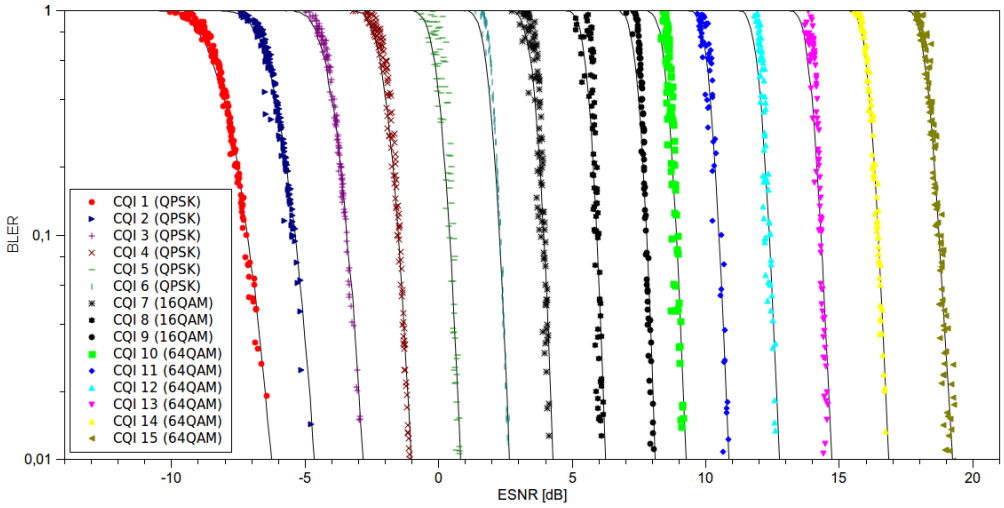

Fig. 15 EESM estimated BLER vs ESNR for HC MIMO (ZF) with CDD in a bandwidth of 4 PRBs and EPA channel

6. Conclusions

The performance of two link abstraction models, MIESM and EESM, has been compared by means of a LTE link level simulator, in a 2x2 MIMO open-loop configuration with CDD and different antenna correlation levels. The models have been trained using a MIMO ZF equalizer with CDD and high antenna correlation because this situation creates high variability of the SINR of the different subcarriers. The obtained parameters can be safely applied for lower antenna correlation levels, for SISO or for MMSE spatial equalization. In turn, MIESM parameters obtained by training the model with a SISO system are not useful to predict the BLER of a MIMO system of the same bandwidth. The interpretation is that in order to obtain valid MIESM parameters with SISO the simulator must use a bandwidth wider than 4 PRBs, so that channel snapshots contain a larger set of different SINR values. Our approach achieves a large set of SINR values per channel snapshot thanks to the CDD, high antenna correlation and ZF combination, thus reducing the simulation time that would be required to simulate a large system bandwidth.

The MIESM model with two parameters must be properly trained to avoid the local minima of the MSE versus the model parameters.

The ESSM model with a single parameter is not able to properly estimate the BLER for 64QAM, but EESM with two parameters achieves an MSE similar to MIESM for all the CQIs. Although MIESM outperforms EESM, the increased precision comes at the cost of computing (or approximating) the MI for all the modulations.

Finally, tables with the MIESM and EESM parameters have been obtained for all the LTE CQIs.

Acknowledgment

This work was supported by the Spanish Ministry of Science under the project TEC2008-06817-C02-02.

References

[1] 3GPP TR 25.892, “Feasibility Study for Orthogonal Frequency Division Multiplexing (OFDM) for UTRAN enhancement”, (Release 6), v6.0.0

[2] K. Brueninghaus, D. Astdlyt, T. Silzert, S. Visuri, A. Alexiou, S. Karger, G. Seraji, “Link Performance Models for System Level Simulations of Broadband Radio Access Systems”, PIMRC 2005

[3] 3GPP2-C30-20030429-010, “Effective-SNR Mapping for Modeling Frame Error Rates in Multiple-state Channels”, Ericsson

[4] X. He, K. Niu, Z. He, J. Lin,” Link Layer Abstraction in MIMO-OFDM System”, IEEE International Workshop on Cross Layer Design 2007

[5] R. Sandanalakshmi, T.G. Palanivelu, K. Manivannan, “Effective SNR Mapping for Link Error Prediction in OFDM Based Systems”, IET-UK International Conference on Information and Communication Technology in Electrical Sciences, ICTES 2007

[6] S. Sesia, I. Toufik and M. Baker, “LTE-The UMTS Long Term Evolution: From Theory to Practice”, Wiley, 2009.

[7] 3GPP TS 36.211, “E-UTRA Physical Channels and Modulation” (Release 8)

[8] 3GPP TS 36.212, “E-UTRA Multiplexing and Channel Coding” (Release 8)

[9] 3GPP TS 36.104, “E-UTRA Base Station (BS) radio transmission and reception” (Release 8)

[10] 3GPP TS 36.213, “E-UTRA Physical layer procedures”, (Release 8)

[11] 3GPP TS 36.101, “E-UTRA UE Radio Transmission and Reception”, (Release 8

[12] J. H. Winters, J. Salz, R. D. Gitlin, "The impact of antenna diversity on the capacity of wireless communication systems", IEEE Transactions on Communications, vol. 42, no. 2, Feb./Mar./Apr. 1994, pp. 1740-1751

[13] F. Adachi, M. Sawahashi, “Performance analysis of various 16 level modulation schemes under rayleigh fading”, IEEE Electronic Letters, 28(17):1579–1581, Aug. 1992

[14] S.Verdú, “Multiuser Detection”, Cambridge University Press, 1998

[15] J. Olmos, A. Serra, S. Ruiz, M. García-Lozano, D. Gonzalez, “Exponential Effective SIR Metric for LTE Downlink”, IEEE International Symposium on Personal, Indoor and Mobile Radio Communications, PIMRC 2009